Spectral identical of Hydrino Compound FeOOH:H_2(1/4) by Five Complementary Spectroscopies

R. Mills[1,2], F. Hagen[3], and M. McKenna[1]

[1]Brilliant Light Power, Inc., 105 Terry Drive, Newtown PA, USA

[2] Corresponding author

[3] Department of Biotechnology, Delft University of Technology, Delft, The Netherlands

ABSTRACT

Mills solves the hydrogen atom and molecule in exact equations that give the experimental observables of both [1]. Uniquely, Mills predicts that in addition to the reciprocal integer squared excited-state electronic energy states of atomic hydrogen, hydrogen possesses integer squared electronic energy levels corresponding to 1/p replacing n in the Rydberg formula, corresponding so-called *hydrino state* of hydrogen. Hydrino, H(1/p), is any small form of atomic hydrogen with state energy $E_n = -13.598/n^2$ eV, in which n = 1/p, and p is a limited by the energy in the electric field of the proton to 126 whereafter the proton and electron decay. Electron transitions to a hydrino states involve an initial non-radiative energy transfer to a catalyst that serves as an energy hole or sink of a quantized amount of energy, $2mE_1$ (m is integer) to be transferred to a catalyst such as HOH, a free or nascent water molecule. Furthermore, hydrino atoms can react to form the corresponding diatomic molecule referred to as molecular hydrino H_2(1/p). In contrast to molecular hydrogen (H_2), the molecular hydrino (H_2(1/p)) is paramagnetic with S = ½, the size is $1/p^3$ that of H_2, the internuclear distance is 1/p that of H_2, and the energies such as the rotational, vibrational, and total molecular energies are p^2 those of H_2. These aspects of H_2(1/p) give rise to unique spectral signatures that are characteristic of and identify H_2(1/p). The recording of unique gas chromatographic (GC), electron paramagnetic resonance (EPR), Raman spectroscopy, electron beam excitation spectroscopy, and X-ray photoelectron spectroscopy (XPS) peaks of H_2(1/4) formed by a high energy impact reaction of FeOOH that served as the source of H and HOH catalyst are reported wherein the observed peaks matched those predicted [1].

Gas Chromatography of $H_2(1/4)$

Ball milling has an effect equivalent to heating to drive chemical reactions [2]. FeOOH was ball milled for 6 hours at 400 RPM intermittently reversing direction using a Retsch PM 100 Planetary ball mill. The ball milling propagated reactions to form $H_2(1/4)$ are

$3FeOOH \text{ to } Fe_3O_4 + H + HOH + 1/2O_2$

$H + HOH_{(catalyst)} \text{ to } H(1/4) + H_2O$

$2H(1/4) \text{ to } H_2(1/4)$

0.5g of the product was placed into a sixty-five-milliliter stainless-steel vessel, 5 ml of concentrated HCl was added to the vessel, and the vessel was vacuum-sealed using a rubber O-ring that set into matching grooves in the vessel and a flanged plate secured to the vessel by six circumferential bolts. One of two valved ports of the plate was connected to the inlet port and a six-way valve to supply gas sample to a pneumatic valve of the gas chromatograph. Using an Agilent 8890 gas chromatograph system with a single filament thermal conductivity detector (TCD), gas chromatography was performed on the gases released by the reaction of iron oxyhydroxide to iron chloride wherein the iron oxide reaction with HCl is

$Fe_3O_4 + 9HCl \text{ to } 3FeCl_3 + 4H_2O + 1/2H_2$

Known gases such as hydrogen, helium, nitrogen, and oxygen were first run to identify their migration times to compare to the results of the FeOOH product sample gas. The pressure controller was set at 35.4 PSI for the flow of argon carrier gas at 3.2 ml/min on a capillary column (Agilent molecular sieve 5 Å, (50 m x 0.32, df = 30 μm) at 303 K (30 °C) with the TCD at 135 °C. The gas inlet injected a 1000 ul sample onto the column wherein the volume was precision-controlled by electronic pneumatic controllers run by compressed nitrogen. The Agilent 8890 system sensed and compensated for atmospheric pressure fluctuations, and a microchannel-based architecture protected against gas contaminants. The data was analyzed using Agilent OpenLab CDS. Hydrogen was confirmed to be a product gas. To add or product gas onto the column, ultrapure hydrogen gas was introduced into the second (intel port) of the vessel and the product gas plus the corresponding hydrogen carrier gas was loaded onto the column by closed inlet valve, opening the outlet value, and then the instrument six-way valve to the column. The gas chromatograph of hydrino gas evolved by room temperature treatment of the FeOOH product for less than one hour is shown in Figure 1. The known hydrogen peak was observed at 4.597 minutes, an oxygen peak was observed at 7.455 minutes, and that nitrogen peak was observed at 13.886 minutes. Two novel peaks were observed before the hydrogen peak at 4.049 minutes and 4.2 minutes. The molecular sieve separates gases by size and weight with hydrogen being the lightest gas that is similar to the other smallest gas, helium. Helium has a retention time slightly greater than that of hydrogen (4.7 minutes). In fact, no gas chromatographic peak has ever been observed before the H_2 peak on a molecular sieve gas chromatographic column. The novel peaks at 4.049

minutes and 4.2 minutes were assigned to para and ortho $H_2(1/4)$, respectively. The property of molecular hydrino peak having a shorter retention time than any known gas was attributed to its decreased molecular size of 64 times geometrically smaller than H_2 and corresponding smaller ballistic cross section.

Figure 1. The gas chromatograph of hydrino gas evolved by acid reaction with ball milled FeOOH that was run within one hour of the acid addition. The two peaks observed at 4.049 minutes and 4.2 minutes before the H_2 peak at 4.597 minutes were assign to p-$H_2(1/4)$ and o-$H_2(1/4)$, respectively.

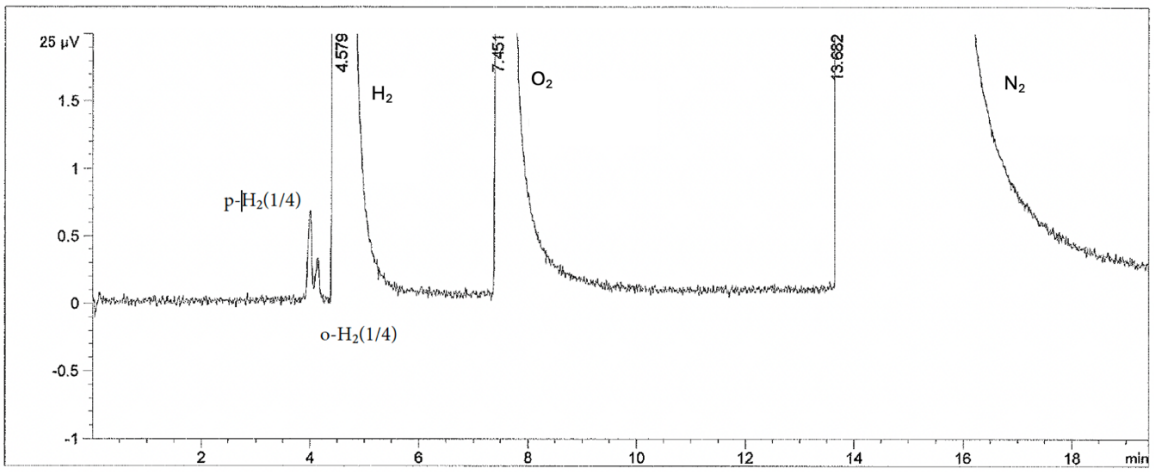

Molecular hydrogen occurs in two nuclear isomeric forms, one with its two proton nuclear spins aligned parallel (orthohydrogen), the other with its two proton spins aligned antiparallel (parahydrogen) [3]. Parahydrogen is in a lower energy state than is orthohydrogen. Ordinally hydrogen ortho para spin isomers may be separated chromatographically at cryogenic temperature such as liquid nitrogen temperature. However, due to the much higher energies of hydrino compared to ordinary hydrogen ortho para hydrogen (See EPR section), may be separated at room temperature. It is also known that the higher energy ortho isomer converts to the more stable para on Fe(III) catalysts such as iron oxide and iron chloride. Overtime more stable para hydrogen is formed at low temperatures. Para hydrogen may be obtained at essentially 100% yield in liquified H_2 in the presence of an iron catalyst. Similarly, it is predicted that ortho $H_2(1/4)$ converts to 100% para form at room temperature upon standing. The gas released initially upon addition of concentrated HCl to ball milled FeOOH showed both ortho and para hydrogen by gas chromatography that converted to 100% para isomeric form upon standing at room temperature for 1 week as shown in Figure 2.

Figure 2. The gas chromatograph of hydrino gas evolved by acid reaction with ball milled FeOOH that was run after one week of the acid addition. Only one peak, the shorter-retention time peak, assign to p-H_2(1/4),was observed at 4.049 minutes before the H_2 peak at 4.597 minutes.

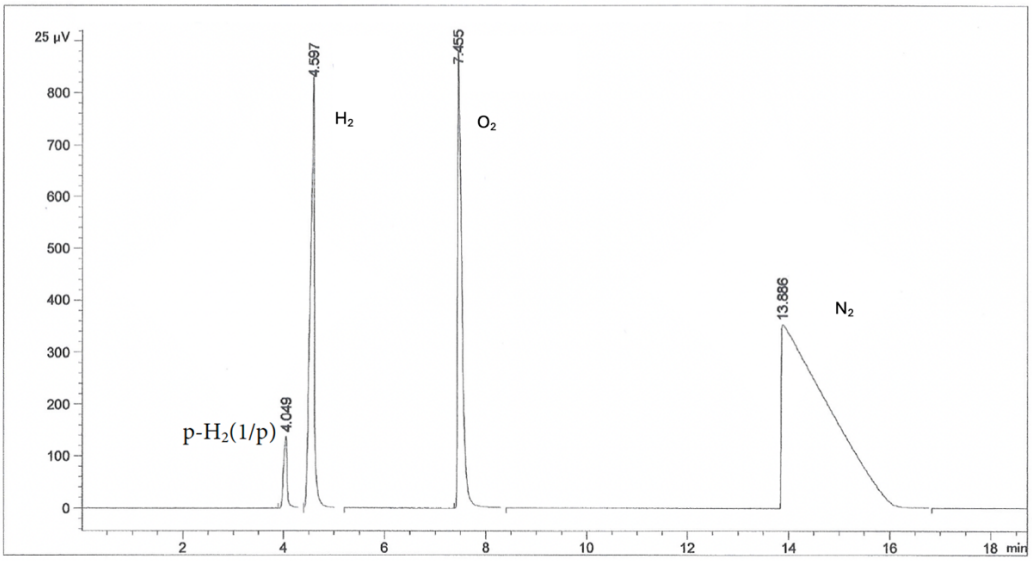

As reported in the Raman section, the series of peaks assigned to H_2(1/4) were eliminated by HCl treatment of the ball milled FeOOH sample. The gas chromatographic results confirm that the source of the Raman peaks was H_2(1/4). The presence of the two spin isomers that catalytically interconvert is further confirmation that the novel peaks with faster migration times tan hydrogen are another form of hydrogen, specifically p-H_2(1/4) and o-H_2(1/4).

Electron Paramagnetic Resonance (EPR) Spectroscopy of H_2(1/4)

The unpair MO electron of H_2(1/p) with a net electron spin of ½ of the H_2(1/p) MO gives rise to spin flip transitions observed by electron paramagnetic spectroscopy (EPR) and well as magnetism observed by magnetic susceptibility measurements [4,5]. EPR was reported on a matrix material Ga(O)OH that had the rare ability to trap individual H_2(1/4) molecules in a gas-like state that allowed for the study of theoretically predicted fine structure in the EPR hydrino signature. Specifically, Hagen and Mills 2022 [4] reported (Figure 3) the theoretically predicted g factor for the spin flip transition with the predicted extraordinary features of a series of multiplets due to fluxon linkage within a series of multiplets due to spin-orbital splitting between the diamagnetic paired and paramagnetic unpaired electron of the MO during the EPR transition. The EPR spectrum of GaOOH@H_2(1/4) was replicated by Bruker using two instruments [6].

Figure 3. The comparison of the EPR spectrum of GaOOH:H_2(1/4) (**A**) and the analytical solution (**B**) of the EPR spectrum of H_2(1/4) comprising spin and orbital coupling multiplets between the paired and unpaired electrons of its molecular orbital and the sub-multiplets due to magnetic flux linkage in integer multiples of h/2e.

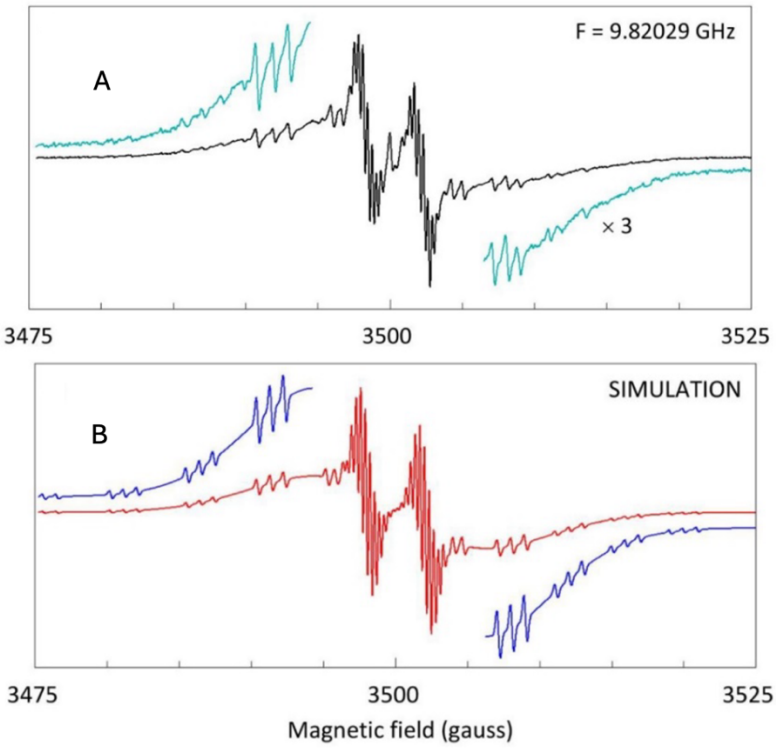

In Hagen and Mills 2024 [5], a large down-field singlet signature and temperature dependencies recorded by EPR were reported that confirm the theoretical prediction of the formation of molecular hydrino dimers $[H_2(1/p)]_2$ as an extension of ordinary hydrogen chemistry. H_2 is known to form dimers $[H_2]_2$ at cryogenic temperatures whereas $[H_2(1/p)]_2$ was shown to be stable at elevated temperatures. Unlike the free-gas H_2(1/4) monomer spectrum of Ga(O)OH@H_2(1/4) shown in high resolution in Figure 4, the dimer $[H_2(1/4)]_2$ EPR spectra were very broad and downfield shifted by 500G.

Figure 4. Two very different types of EPR spectra were observed from molecular hydrino samples, ZnO@H_2(1/4) prepared by Zn wire detonation in humidified air atmosphere (blue trace) and Ga(O)OH@H_2(1/4) prepared by aqueous KOH treatment of gallium oxide collected following a plasma reaction in a SunCell [6] comprising molten gallium as one of the electrodes (red trace).

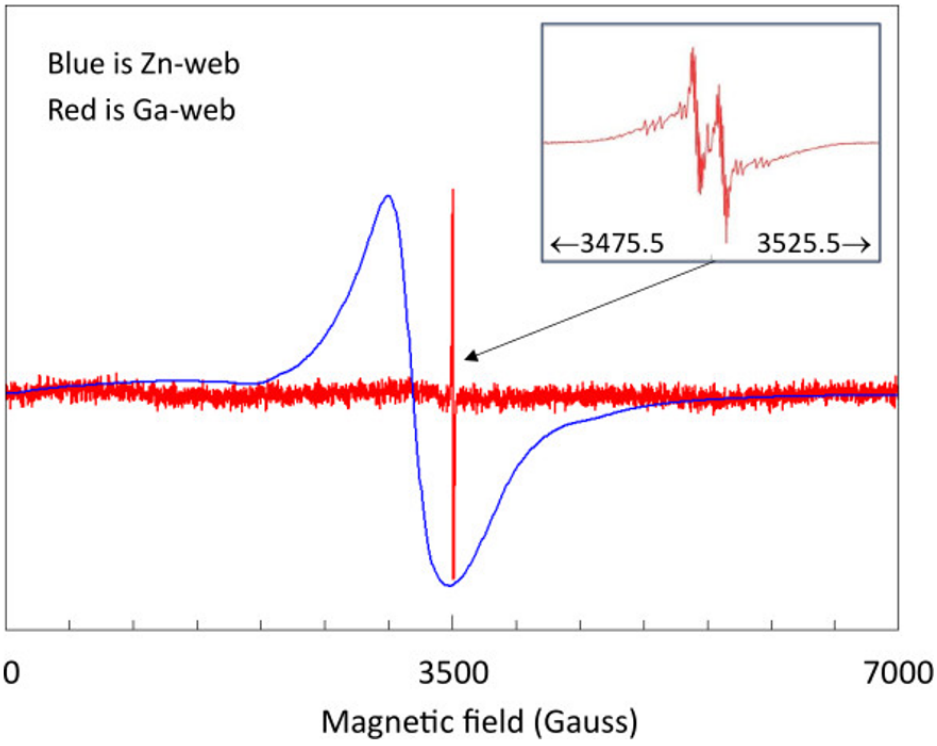

Moreover, at low temperatures, it was observed that $[H_2(1/4)]_2$ dimers side to side anti-paired to form tetramers that were not EPR active. As the temperature was raised the EPR singlet for the dimer reappeared at the predicted temperature. The results further show the production of H_2(1/8) and $[H_2(1/8)]_2$ dimers indicating greater release of energy than production of H_2(1/4). The observation of the formation of a dimer between molecular hydrino H_2(1/4) and H_2 ([H_2-H_2(1/4)]) and the temperature dependence of hydrogen release explains the massive amounts of hydrogen observed from salts containing molecular hydrino reported previously [6].

FeOOH:H_2(1/4) was prepared by ball milling FeOOH for 6 hours at 400 RPM intermittently reversing direction using a Retsch PM 100 Planetary ball mill. The EPR spectrum of ball milled FeOOH shown in Figure 5 matches that of other samples comprising dimers

$[H_2(1/p)]_2$ (Figure 4) wherein the predicted dimer shift of 502 G and a peak width of 335 G were observed [5].

Figure 5. $[H_2(1/p)]_2$ EPR spectrum of FeOOH:$H_2(1/4)$ showing the predicted extreme downfield shifted and broadened peak.

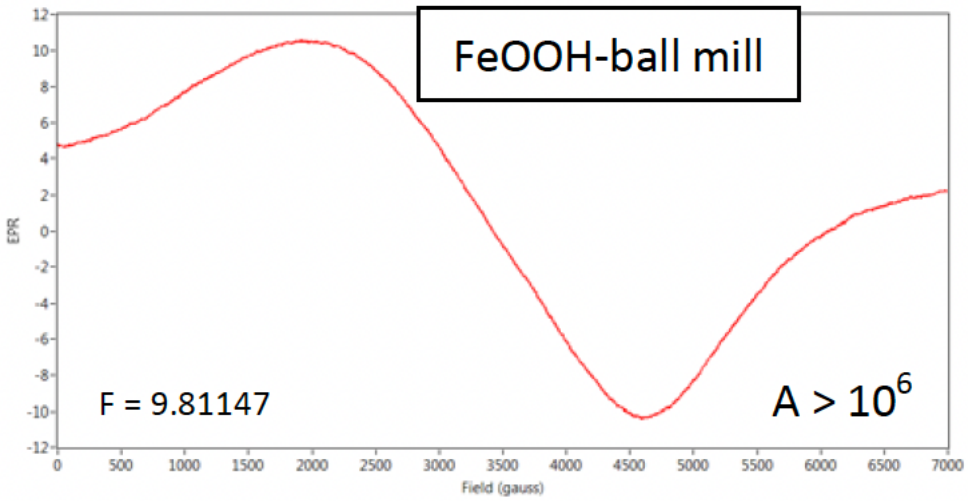

785 nm anti-Stokes and Stokes Raman Spectroscopy

Molecular hydrino such as $H_2(1/4)$ of a composition of matter such as FeOOH@$H_2(1/4)$ may undergo two-photon absorption to excite a rotational energy state and it spin-orbital and fluxon linkage fine structure observed by EPR (Figure (3)) wherein the excited states may decay as a single photon. FeOOH@$H_2(1/4)$ was prepared by ball milling FeOOH. The 785 nm anti-Stokes and Stokes spectra recorded with a Horiba Jobin Yvon LabRAM Aramis Raman spectrometer using the 300 mW 785 nm laser and 600 line/mm grating are shown in Figures 6-8. The series of peaks match a $H_2(1/4)$ rotational transition with spin orbital coupling and fluxon linkage fine structure with assignments given by Mills [6]. The series of Raman peaks recorded on FeOOH@$H_2(1/4)$ are eliminated by HCl treatment that releases H_2 and $H_2(1/4)$ gas [6]. To further test the two-photon excitation mechanism, the spectra were obtained at 100X objective with the power varied from 25% to 50% wherein it was found that the series of peaks was not observed at 25% laser power but was observed at 50% laser power. The anti-Stokes and Stokes spectra are remarkable in that the energy ranges are higher than any prior recorded, there is a threshold laser intensity to observe the emission lines, and the first, second, and third order peaks are observed that match the rotational transitions of $H_2(1/4)$ and not any known source. The Raman results provide strong confirmation of $H_2(1/4)$ and the two-photon excitation mechanism

of the rotational energy levels of $H_2(1/4)$. The results further demonstrate the two-photon rotational excitation mechanism for $H_2(1/4)$ embedded in a powdered magnetic metal oxide matrix that gives rise to spin-orbital and fluxon linkage transitional fine structure. Spin-orbital and fluxon linkage fine structure of the Raman spectrum matches those of the EPR (Figure 3) and electron beam excitation emission (Figure 9) spectral results.

Figure 6. Raman anti-Stokes (-50 cm^{-1} to -8000 cm^{-1}) and Stokes (100 cm^{-1} to 8000 cm^{-1}) of the ball milled FeOOH sample recorded with 25% and 50% 300 mW 785 nm laser power and 100X objective. The anti-Stokes emission is the source of the Stokes-spectral lines assigned to second and third order high-energy emission.

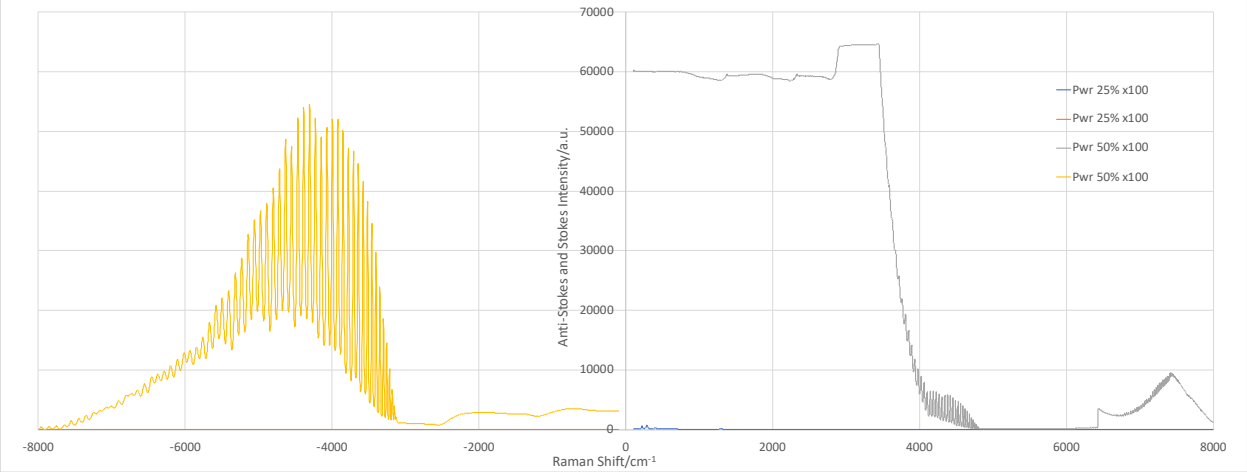

Figure 7. Raman anti-Stokes (-50 cm^{-1} to -8000 cm^{-1}) of the ball milled FeOOH sample recorded with 25% and 50% 300 mW 785 nm laser power and 100X objective.

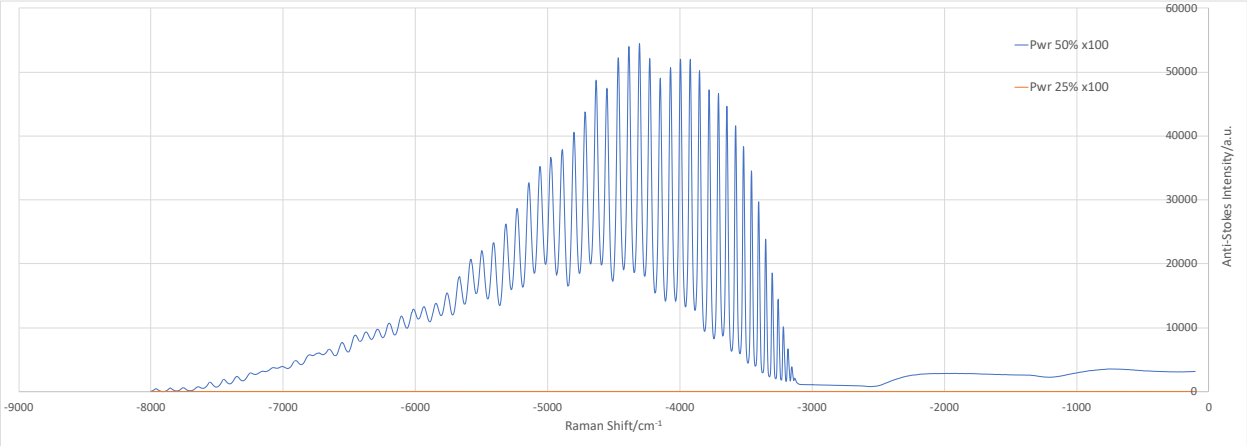

Figure 8. Raman Stokes (100 cm^{-1} to 8000 cm^{-1}) of the ball milled FeOOH sample recorded with 25% and 50% 300 mW 785 nm laser power and 100X objective.

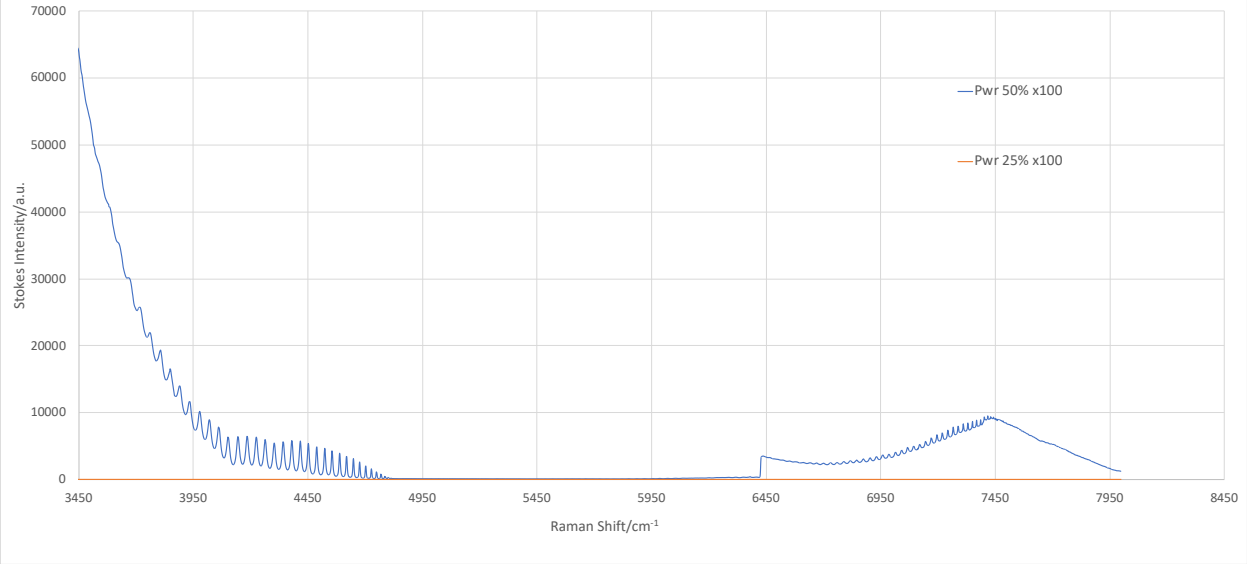

Electron Beam Excitation Emission Spectroscopy

The ro-vibration band of $H_2(1/4)$ was shown by electron beam excitation spectroscopy of $H_2(1/4)$ gas released from heating FeOOH:$H_2(1/4)$ wherein the pressure was brought up to atmospheric by addition of argon gas. The argon gas was initially allowed to stand at atmospheric pressure and 300K for two days to remove any $H_2(1/4)$ gas by diffusion and was added to enhance the $H_2(1/4)$ emission in the spectral region of the ro-vibrational band of H2(1/4) by a known resonance energy transfer from the argon excimer band [6]. The chamber gas was excited by a 12 keV to 16 keV electron-beam incident the gas through a silicon nitride window. The emission was observed through a MgF_2 window on the opposite side of the gas chamber relative to the silicon nitride window. Emission from the electron-beam excitation was recorded using a McPherson grazing incidence EUV spectrometer (Model 248/310G) equipped with a platinum-coated 600 g/mm or a platinum-coated 1200 g/mm grating. The angle of incidence was 87°. The wavelength resolution was about 0.05 nm with an entrance slit width of <1 μm. The EUV light was detected by a CCD detector (Andor iDUS Model #: DO420A-BEN-995, Serial #: CCD-24974, Date: 2020) cooled to -60 °C. As shown in Figure 9, the ro-vibrational spectrum of $H_2(1/4)$ was observed as emission lines in the ultraviolet region (130-200 nm) by 12-16 keV electron beam excitation FeOOH:$H_2(1/4)$ decomposition gas. A series of equal, 0.25 eV spaced line emission was in the ultraviolet (150-180 nm) region with a cutoff at 8.2 eV that matched the $H_2(1/4)$ $\nu = 1$ to $\nu = 0$ vibrational transition with a series of rotational transitions corresponding to the $H_2(1/4)$ P-branch. The spectral fit was a good match to $4^2 0.515eV - 4^2\left(J+1\right)0.01509; J = 0,1,2,3\ldots.$ wherein 0.515 eV and 0.01509 eV are the

vibrational and rotational energies of ordinary molecular hydrogen, respectively, further confirming the Raman assignments. The R-branch is not expected to be observed due to the lack of population of ro-vibration states with the plasma gas temperature being lower than the ro-vibrational excitation temperature. The fine structure in the spectrum is due to spin-orbital splitting observed in the EPR (Figure 3) and Raman (Figures 6-8) spectra.

Figure 9. Ultraviolet emission spectrum from electron beam excitation of $H_2(1/4)$ gas released from heating FeOOH:$H_2(1/4)$ and mixed with atmospheric pressure argon gas absent $H_2(1/4)$ gas. The cutoff of 8.2 eV and the line spacing of 0.25 eV matched the $\upsilon = 1$ to $\nu = 0$ vibrational transition with the P-branch rotational spectrum of $H_2(1/4)$.

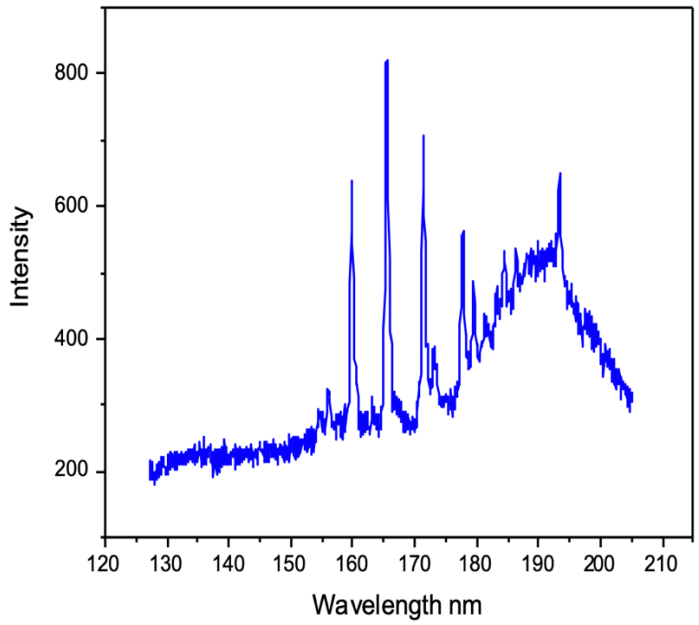

X-ray Photoelectron Emission Spectroscopy (XPS)

FeOOH was ball milled for 6 hours at 400 RPM intermittently reversing direction using a Retsch PM 100 Planetary ball mill. XPS was recorded with a Kratos Axis Ultra XPS using a Al K-alpha X-Ray source, a pass energy of 120 eV, and a step size of 1.0eV. C1s was calibrated to 284.8eV. A broad peak at 496 eV (Figure 10) was assigned to $H_2(1/4)$ wherein other possibilities such Na, Sn, and Zn were eliminated since the corresponding peaks of these candidates are absent. The peak intensity was as expected due to the small cross section of $H_21/4)$ that comprises only two electron with a size 64 times smaller than H_2. Other elements present were Fe, C, and O wherein two different chemical states of O were observed as shown by the two O1s peaks in 531

eV region. The 496 eV peak assigned to $H_2(1/4)$ and the two chemical states of oxygen were also observed in the XPS spectrum of GaOOH [6].

Figure 10. The XPS spectrum of ball milled FeOOH showing the H2(1/4) total energy peak at 496 eV as well as two chemical states of O as indicated by the O1s peaks.

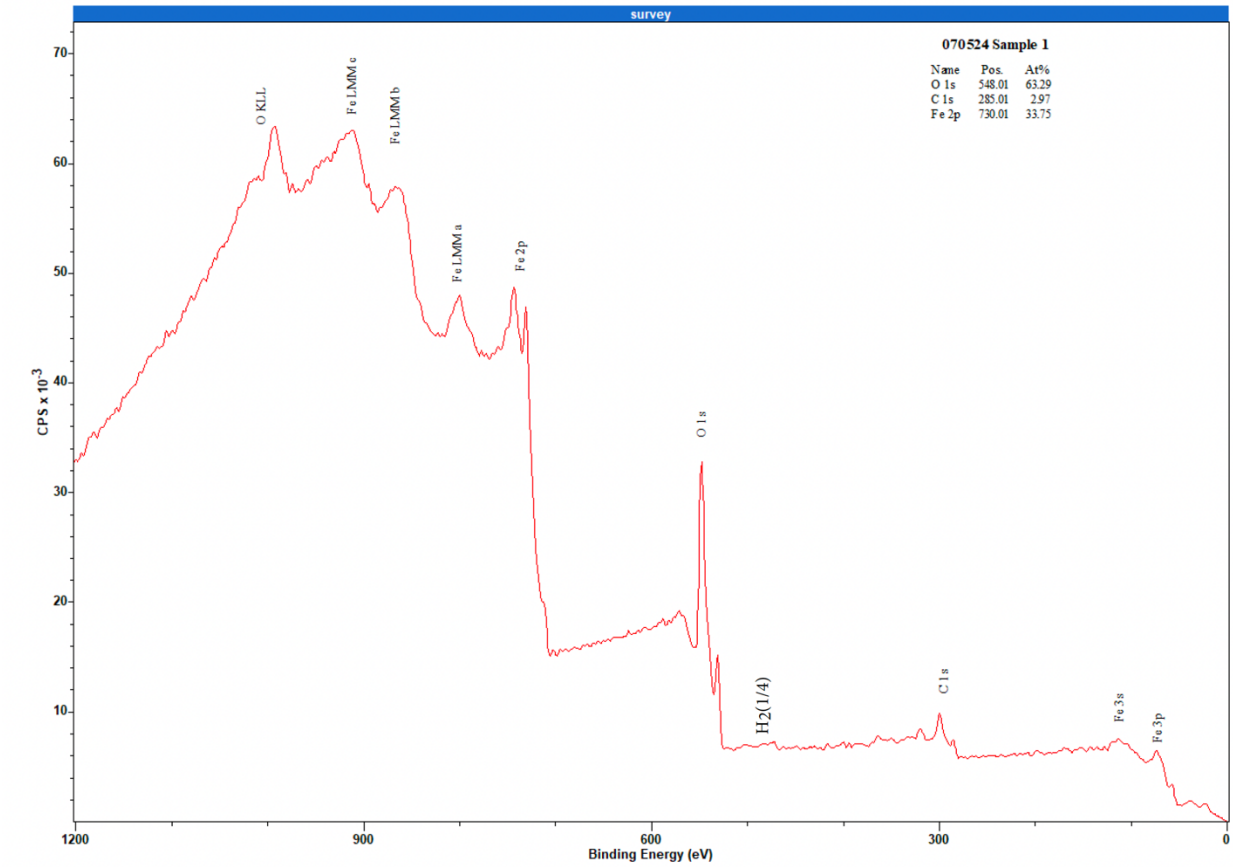

References

1. R. Mills, The Grand Unified Theory of Classical Physics, April 2023 Edition, ISBN 979-8-218-17988-5, Library of Congress Control Number 2023905641, https://brilliantlightpower.com/GUT/GUT-CP-2020-Ed-Web.pdf
2. T. Markmaitree, R. Ren, L. L. Shaw, "Enhancement of lithium amide to lithium imide transition via mechanical activation", J. Phys. Chem. B., Vol. 110, No. 41, pp. 20710-20718.
3. https://en.wikipedia.org/wiki/Spin_isomers_of_hydrogen#:~:text=2-,,cause%20significant%20loss%20by%20boiling.
4. Wilfred R. Hagen, Randell L. Mills, "Electron Paramagnetic Resonance Proof for the Existence of Molecular Hydrino", Vol. 47, No. 56, (2022), pp. 23751-23761; https://www.sciencedirect.com/science/article/pii/S0360319922022406.

5. Wilfred R. Hagen, Randell L. Mills, “General EPR pattern from molecular hydrino produced in various reactors”, (2024), submitted; https://brilliantlightpower.com//pdf/General_EPR_pattern_from_molecular_hydrino_produced_in_various_reactors.pdf.
6. R. Mills, “Hydrino States of Hydrogen”, https://brilliantlightpower.com/pdf/Hydrino_States_of_Hydrogen_Paper.pdf, submitted for publication.